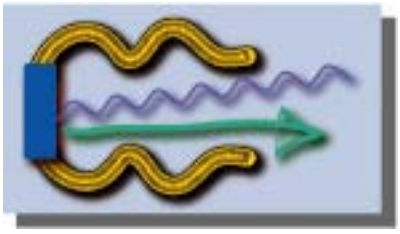

PHIN

Design and testing of amplifiers for the CTF3 photo-injector laser

M. Divall, G. Kurdi, I. Musgrave, E. Springate, W. Martin, G.J. Hirst and I.N. Ross
Central Laser Facility, CCLRC Rutherford Appleton Laboratory, Chilton, Didcot, Oxon., OX11 0QX
V. Fedosseev, N. Champault, G. Suberlucq and R.Losito
CERN, Geneva, Ch-1211 23 Switzerland

Abstract

We present the design and preliminary test results for the two diode-pumped Nd:YLF amplifiers of the CTF3 photo-injector. These are designed to amplify a 1.5 GHz train of pulses to provide 3 kW pulse-train mean power in a 400 μs macropulse after the first amplifier and 15 kW in a 200 μs macropulse after the second. Tests of the first amplifier show good agreement with our calculations, with the output power exceeding 3.3 kW.

Work supported by the European Community-Research Infrastructure Activity under the FP6 « Structuring the European Research Area » programme (CARE, contract number RII3-CT-2003-506395).

Design and testing of amplifiers for the CTF3 photo-injector laser

M. Divall, G. Kurdi, I. Musgrave, E. Springate, W. Martin, G.J. Hirst and I.N. Ross

Central Laser Facility, CCLRC Rutherford Appleton Laboratory, Chilton, Didcot, Oxon., OX11 0QX

V. Fedosseev, N. Champault, G. Suberlucq and R.Losito

CERN, Geneva, Ch-1211 23 Switzerland

Abstract

We present the design and preliminary test results for the two diode-pumped Nd:YLF amplifiers of the CTF3 photo-injector. These are designed to amplify a 1.5 GHz train of pulses to provide 3 kW pulse-train mean power in a 400 μs macropulse after the first amplifier and 15 kW in a 200 μs macropulse after the second. Tests of the first amplifier show good agreement with our calculations, with the output power exceeding 3.3 kW.

Introduction

The CTF3 photo-injector laser system is designed to deliver high power, microsecond long trains of ultraviolet laser pulses. The 1.5 μs pulse trains (macropulses) each contain ~2300 micropulses, at a 1.5 GHz repetition rate. The system will run at up to 50 Hz macropulse repetition rate, delivering 15 kW pulse train mean power in the IR. This light will then be converted into the UV. The system requirements are shown in Table 1.

Target Parameters	Units	CTF3
Electron charge / bunch	nC	2.33
Number of pulses per macropulse	-	2332
Oscillator repetition rate	GHz	1.5
Macropulse width	μs	1.548
Macropulse repetition rate	Hz	5/50
Cathode wavelength	nm	262
Energy at cathode per pulse	nJ	370
IR/UV conversion efficiency	%	7.4
IR energy per pulse	μJ	10
IR pulse train mean power	kW	15
IR average power (at 50 Hz)	W	200
UV average power (at 50 Hz)	mW	86
Amplitude stability	%	<0.25

Table 1. *System requirements for CTF3 Photo-injector laser.*

System description

The layout of the whole laser system is shown in figure 1. A Nd:YLF passively mode-locked oscillator and CW preamplifier system has been purchased [1], producing 6 ps pulses at a 1.5 GHz repetition rate at 1047 nm with an average power of 320 mW after the oscillator and 10 W after the preamplifier. The oscillator and pre-amplifier can be synchronised to an external reference source with a time jitter <1ps. A high speed fibre modulator will be placed between the laser oscillator and preamplifier system to allow phase coding of the 1.5 GHz pulse train. The fibre-coding hardware is intrinsically lossy, with an estimated power loss of 10 dB, and preliminary measurements indicate that this will reduce the output to ~6 W.

The output of the oscillator and preamplifier system will then be amplified in a series of two Nd:YLF diode-pumped power amplifiers. In the first amplifier, we pump with 15 kW of diode power in 400 μs pulses to reach a pulse-train mean power of 3 kW (2 μJ per micropulse). The second amplifier, where we pump with 20 kW of diode power in 200 μs pulses, has a gain of five to give an output pulse-train mean power of 15 kW. The output pulse trains are then

gated with a fast Pockels cell to produce 1.55 μs, flat-top pulse trains, before second and then fourth harmonic generation.

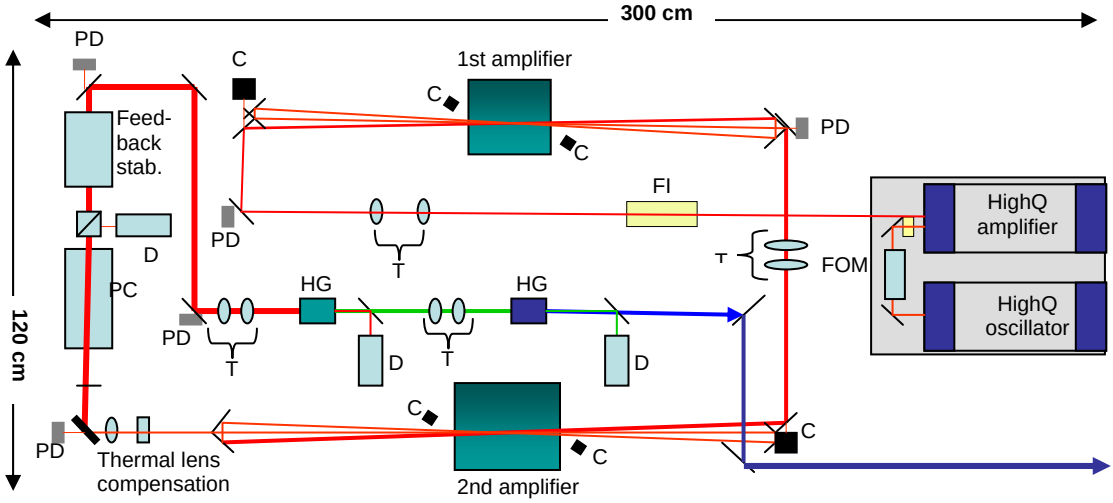

Figure 1. *Layout of the laser system. FOM, fibre-optic modulator, FI, Faraday isolator; T, telescope; PD, calibrated photodiode for power monitoring; C, camera to monitor alignment; PC, Pockels cell to produce 1.55 μs flat-top pulse train; D, diagnostics; HG, harmonic generation crystal.*

Laser head design. The amplifier heads are based on side-pumped Nd:YLF rods, with five diode bars equally spaced around the circumference of the rod. The laser head mechanics have been designed and manufactured at RAL. To achieve homogeneous pumping along the length of the rod, the design is based on long vertical stacks of diode bars, which match the length of the Nd:YLF rods. The fast axis divergence of 40° assures the filling of the rod along the optical axis while the 10° slow axis divergence is corrected by long cylindrical lenses to match the cross-section of the rod. A glass tube contains the coolant for the laser rod. The expected overall coupling and absorption efficiency in the rod is ~70%. The rod mounting system allows easy rotation of the naturally birefringent rods to suit the input polarization and interchange of the rods (figure 2a). The head of the first amplifier has been manufactured, assembled and tested (figure 2b). The second amplifier head, which is essentially a scaled-up version of the first, has been designed and is currently being manufactured. The parameters of the amplifier heads are listed in Table 2.

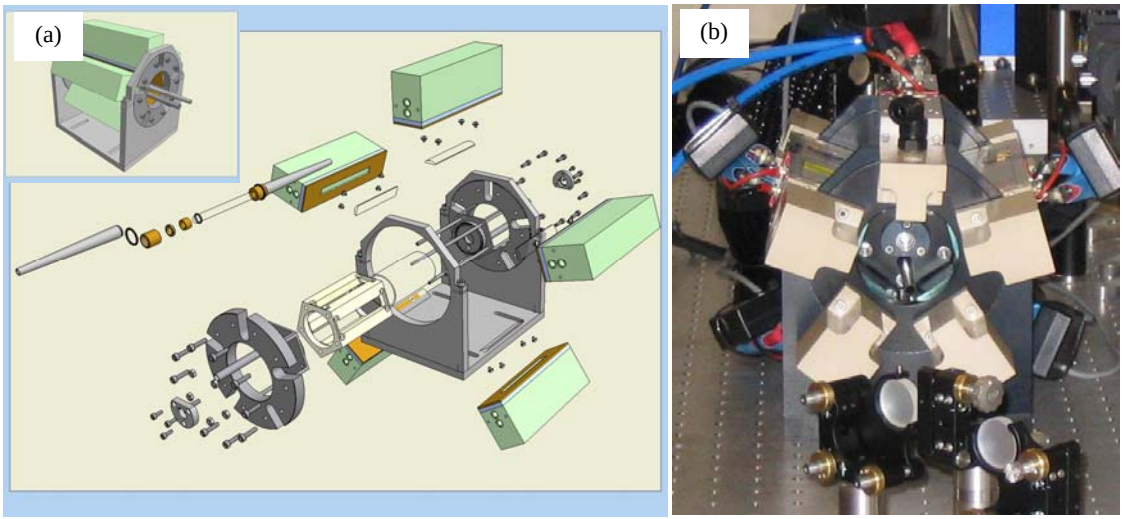

Figure 2. *(a) Amplifier head assembly and (b) the assembled first amplifier head.*

While Nd:YLF is in many respects an ideal laser material for this application, its major disadvantage is the low thermal fracture limit at a thermal load of ~18 W/cm. We are

collaborating with MPQ to test a variety of crystals with different surface treatments from a number of manufacturers to measure the fracture limit. The low thermal fracture limit means that it is important to pump the rod as uniformly as possible. The chosen supplier for the diodes for both amplifiers was Dilas Diodenlaser GmbH. The diodes are pre-assembled, uniformly spaced diode arrays to minimise the assembly and testing time and also to maximise the pumping uniformity at the rod. The five diode stacks for the first amplifier consist of stacks of 36 diodes, evenly spaced with a 1.95 mm vertical bar-to-bar pitch, emitting area of 70x11 mm and a power per stacked array of 3600 kW. Those for the second amplifier consist of stacks of 44 diodes, evenly spaced with a 2.5 mm vertical bar-to-bar pitch, emitting area of 110x11 mm and a power per stacked array of 4400 kW. The diode wavelength of 802±2 nm was chosen because of the low variation of absorption with wavelength in this region. As diode wavelength varies with temperature, this increases the stability of the system. The diodes for both amplifiers require substantial cooling systems, with 45 litres/min of deionised water at 2.5 bar for the first amplifier and 66 litres/min at 3.2 bar for the second. We control the temperature stability of the cooling water to ±0.1 K to maintain the stability of the laser output as measurements on the PILOT amplifier showed that raising or lowering the cooling water temperature by 0.5 K changed the output laser energy by 5% [2].

	1st amplifier	**2nd amplifier**
Length of the rod	8 cm	12 cm
Diameter of the rod	7 mm	10 mm
Effective pump length	7 cm	11 cm
Total peak pumping power	18 kW	25 kW
Repetition rate	1-50 Hz	1-50 Hz
Max. duty cycle	2.5%	2%
Max. average pumping power	450 W	500 W
Cooling requirement	45 l/min	66 l/min
Number of passes	3	3
Expected gain	300	5

***Table 2**. Amplifier head parameters.*

The diodes are driven by Laselec LYDYA diode drivers, designed for QCW operation with short rise and fall times and <1% overshoot. These are controlled by LabView software which enables the current through each of the five diodes to be set and error messages monitored.

Amplifier design. The amplifier design is based on a quasi steady-state operation, because of the high stability required. The model is discussed in detail in [3]. Figure 3 shows the calculated gain in the two amplifiers as a function of pumping duration, with the diodes in the second amplifier switched on 125 μs after those for the first amplifier. It can be seen that the steady state, where the total gain is constant in time, is reached after ~250 μs. We then slice out a section of this steady-state output with a Pockels cell to give a 1.55 μs flat-top pulse train. An alternative 'burst-mode' solution, where the 1.5 GHz output of the oscillator and pre-amplifier would be chopped to give few-microsecond trains of pulses which are then amplified, was also considered. Amplified flat-top pulse trains have previously been demonstrated with this technique [4]. In this burst mode, less diode pumping time is required. The energy per pulse (peak power) obtainable from the amplifier depends on the pump power, so the diode power would need to be the same to get the same output peak power. However, diode duty cycles are standardised, and diode lifetime depends on the number of shots, not the energy per pulse. Reducing the diode pumping time would not, therefore, reduce the cost of the diodes. Running with shorter diode pulses would help with thermal management, but in our steady-state design we can get enough gain while remaining well below the fracture limit, so this is not a problem. With steady-state operation the output is more stable against slow input variations, while if the diodes ran with shorter pulses these input variations could cause high gain overshoot at the front of the train. Sophisticated feedback stabilization and timing

control would therefore be needed for safe operation, making the steady-state solution the preferred option.

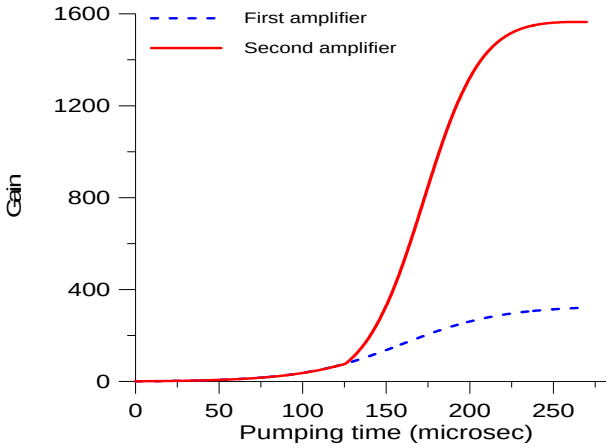

Figure 3 *Calculated gain in the two amplifiers. The diodes in the first amplifier are switched on at 0 μs and the second amplifier is switched on 125 μs later. The dotted blue line shows the gain in the first amplifier and the red line the gain in both amplifiers together. It can be seen that the steady-state, where the gain is constant in time, is reached after 250 μs.*

Amplifier performance

Pumping uniformity. Figure 4 shows the fluorescence distribution in the rod for pumping with individual diode arrays and with all five diode arrays together. The rod sees diode radiation with mixed polarisations both parallel and perpendicular to the c-axis. The absorption parallel to the c-axis is a factor of two higher than perpendicular, making it difficult to calculate the pumping distribution. The effect of the diode polarisation is visible, with the diodes closest to the horizontal (Fig 4 c,d) being most strongly absorbed. When we pump with all five diodes, the five-fold geometry and slight offset of each diode from the centre-line of the rod enable us to obtain a pumping uniformity of nearly 80% over the total area of the rod.

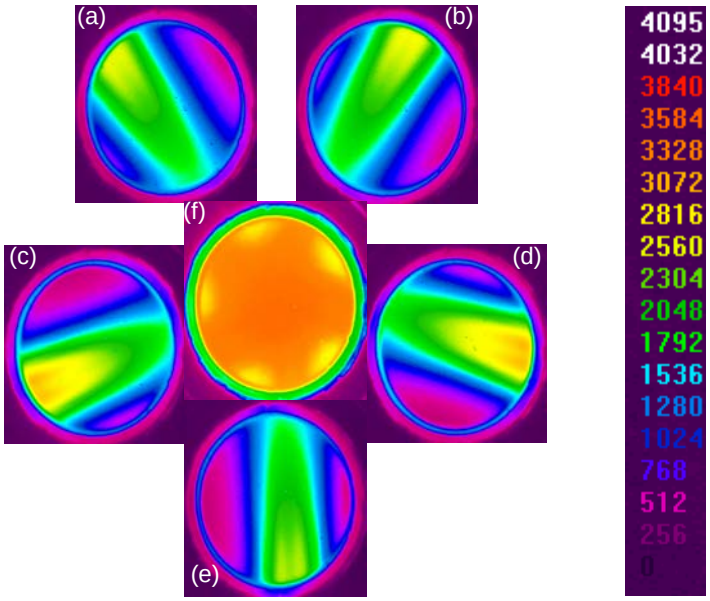

Figure 4 *Measured fluorescence distribution from each of the five diodes individually (a-e) and from all five diodes together (f).*

Single pass performance. We have measured the gain of the first amplifier in single pass and compared the results against the predictions of the code [3]. The measured and calculated single-pass gains obtained with input powers of 200 mW and 6800 mW are shown in figures 5 and 6 respectively. The measurements show good agreement with the code, except at the highest input and pump powers (figure 6f) when the measured gain is ~80% of that predicted. This discrepancy between the code and measurements suggests that the model for ASE used in the code is not correct. However, we do still obtain sufficient gain. With the design values of 6800 mW input power and 15.8 kW pump power, we measure a single-pass gain of >200.

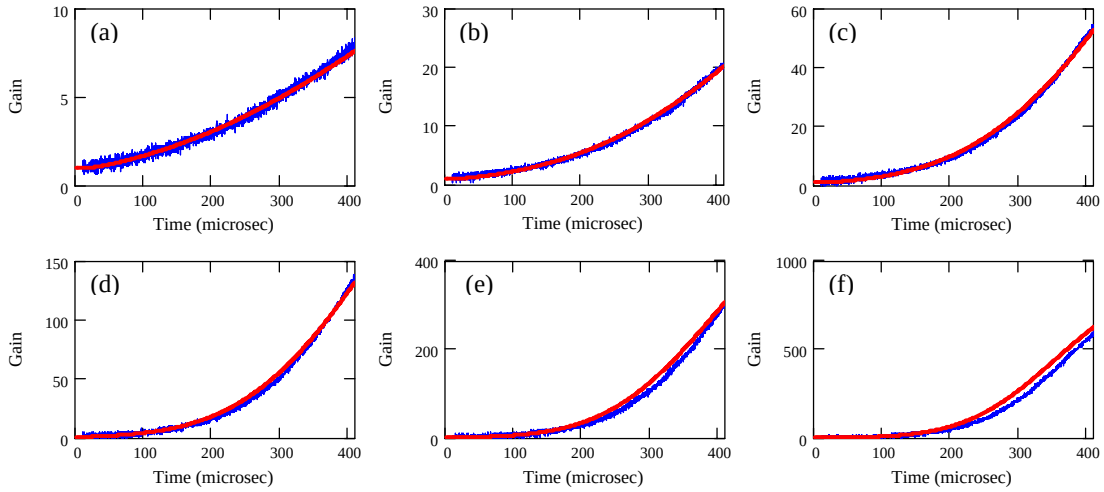

Figure 5 *Measured (blue) and calculated (red) single pass gain with pump powers of (a)4.7 kW, (b) 6.9 kW, (c) 9.2 kW, (d) 11.4 kW, (e) 13.6 kW and (f) 15.8 kW. The input power was 200 mW.*

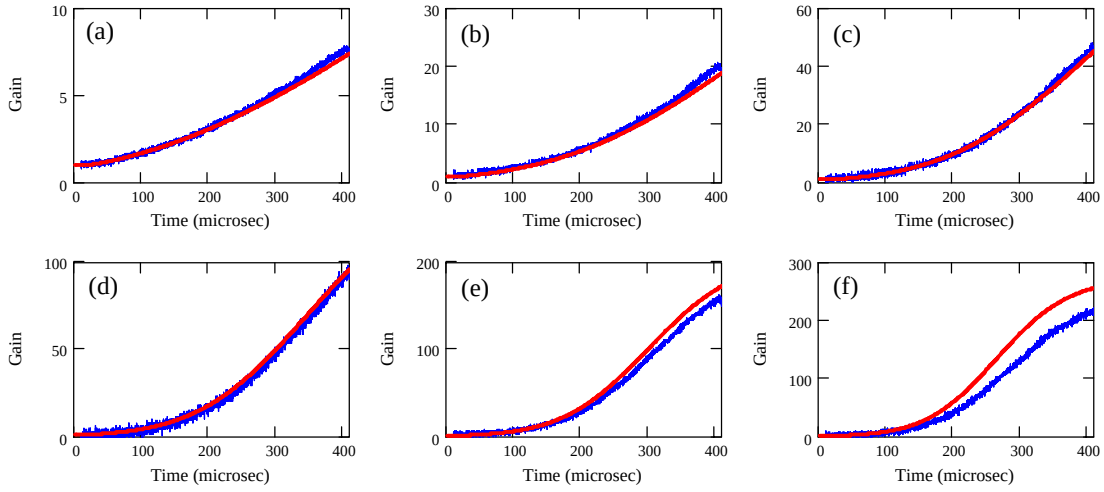

Figure 6 *Measured (blue) and calculated (red) single pass gain with pump powers of (a) 4.7 kW, (b) 6.9 kW, (c) 9.2 kW, (d) 11.4 kW, (e) 13.6 kW and (f) 15.8 kW. The input power was 6800 mW.*

Multi-pass performance. The amplifier is designed to run with three passes of the rod (as shown in figure 1) and this multi-pass configuration has also been assembled and tested. We use a telescope to focus weakly into the rod, giving beam diameter of 1 mm in the rod at the first pass. The beam then expands through the amplifier to give beam sizes of 2 mm and 3 mm on the second and third passes respectively. The measured gain after three passes of the amplifier for input powers of 130 mW and 6300 mW respectively are shown in figures 7 and

8. At the full input power and diode pump power, the gain saturates at 525 after 300 μs giving an output power of 3390 W. This compares well with the design input power to the second amplifier of 3 kW.

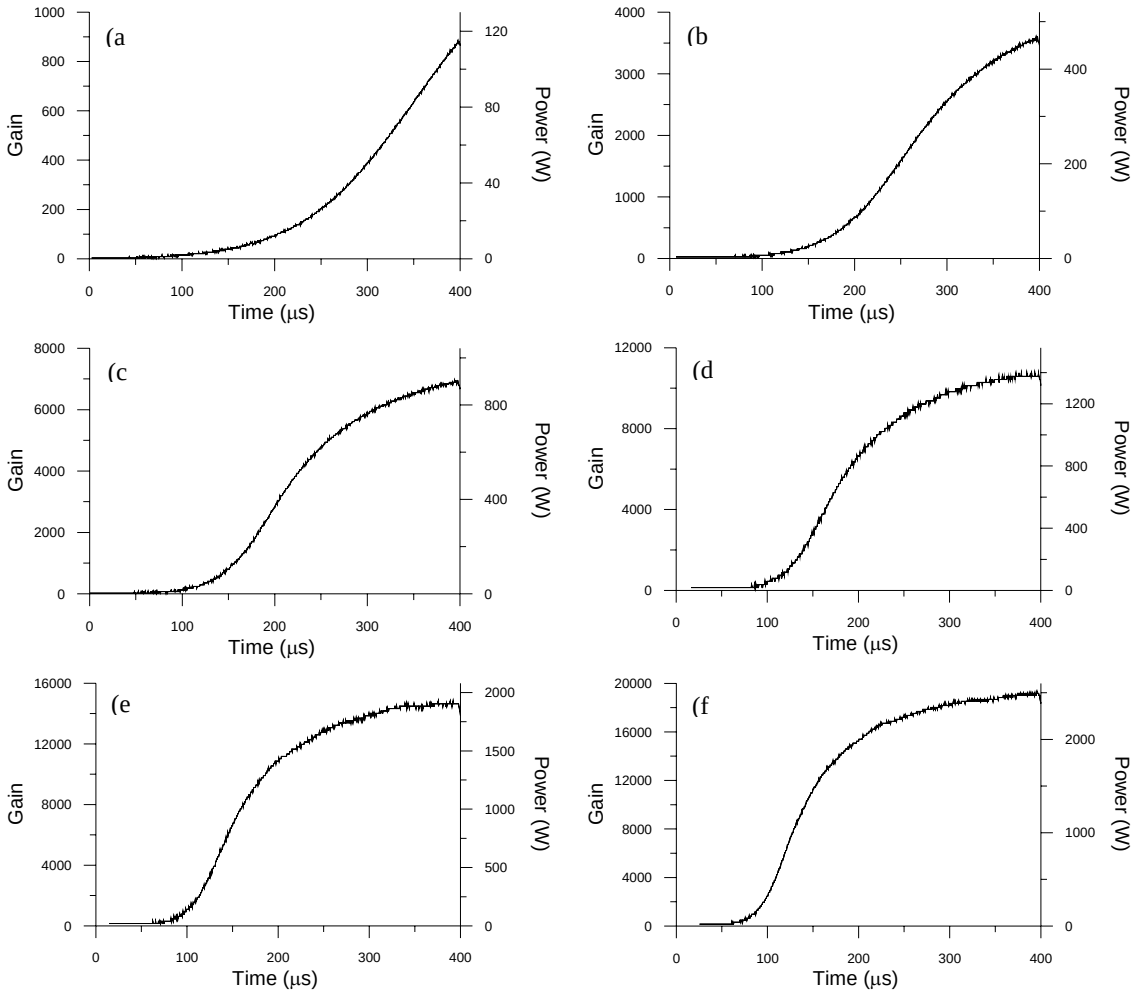

Figure 7 *Measured gain after three passes with pump powers of (a) 4.7 kW, (b) 6.9 kW, (c) 9.2 kW, (d) 11.4 kW, (e) 13.6 kW and (f) 15.8 kW in total. The input power was 130 mW.*

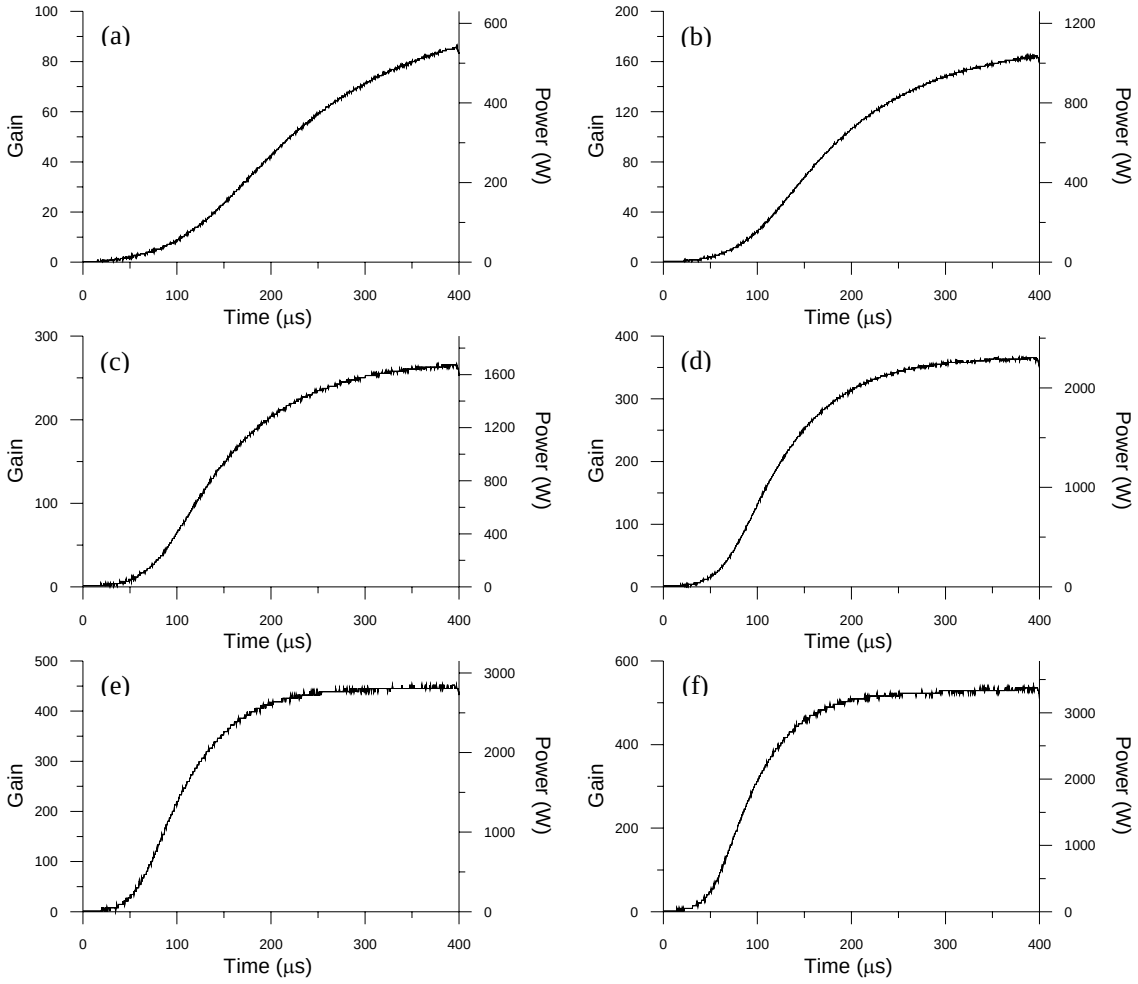

Figure 8 *Measured gain after three passes with pump powers of (a) 4.7 kW, (b) 6.9 kW, (c) 9.2 kW, (d) 11.4 kW, (e) 13.6 kW and (f) 15.8 kW in total. The input power was 6300 mW.*

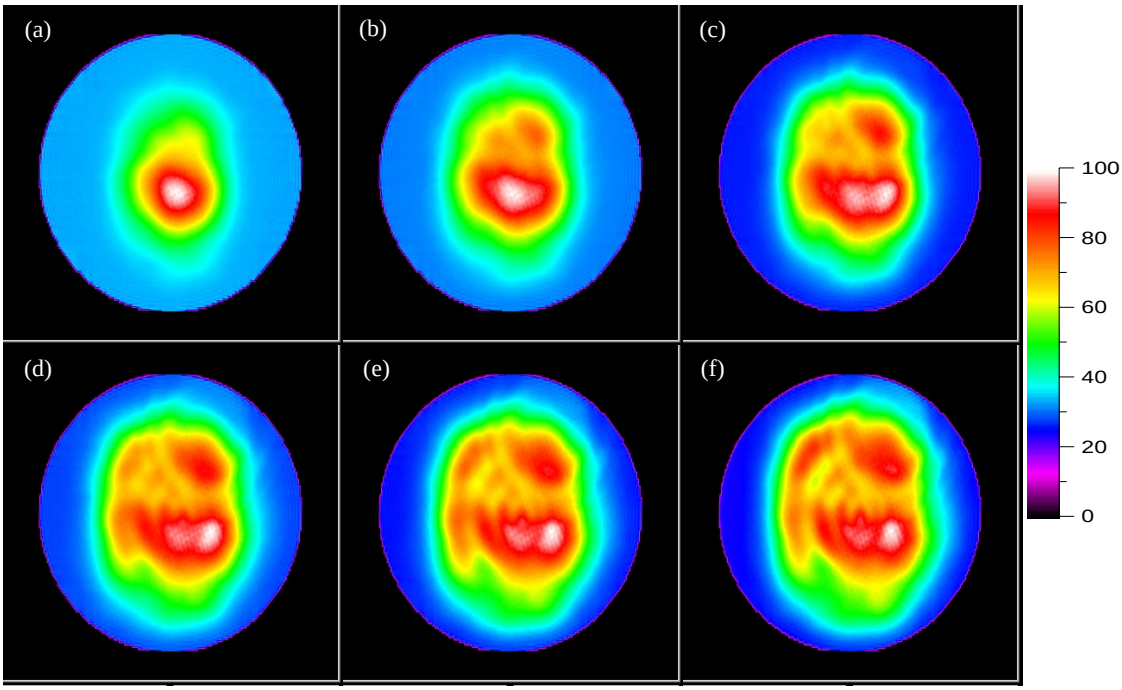

Figure 9 *Measured beam profiles after three passes in the amplifier with pump powers of (a) 4.7 kW, (b) 6.9 kW,(c) 9.2 kW, (d) 11.4 kW, (e) 13.6 kW and (f) 15.8 kW in total. The input power was 130 mW.*

We have also measured the beam profiles after three passes of the amplifier for pump powers ranging from 4.7 kW to 15.8 kW, as shown in Figure 9. The beam diameter increases with increasing pump power due to saturation. The beam profile is affected by inhomogeneities in the Nd:YLF rod, but is acceptably smooth.

Thermal lensing. One important advantage of Nd:YLF is its weak thermal lens compared to other solid state laser media, such as Nd:YAG [5]. The thermal time constant, τ, of the rod, given by r^2/κ where r is the rod radius and κ the thermal diffusivity, is 6 s for the first amplifier. The time between pulses is so short compared to τ that essentially no temperature decay takes place between pulses. The temperature profile is then identical to that obtained at CW operation for the same input power. Assuming uniform pumping along the length of the rod and around its circumference, this sets up a temperature profile which is highest in the centre of the rod and decreases quadratically with radius [6]. With 10 litres/min cooling water flow, we calculate a temperature difference between the centre and edges of the rod of 16 °C at 50 Hz operation.

The two major contributions to the thermal lens are the change in refractive index and length of the rod with temperature. Stress-induced birefringence is not believed to be a major contributor to thermal lensing in Nd:YLF because of the large natural birefringence [7]. The change in refractive index with temperature, dn/dT, is negative and different along each of the two axes ($dn_a/dT = -4.3\times10^{-6}$ °C^{-1}, $dn_c/dT = -2\times10^{-6}$ °C^{-1}), so the contribution from this gives a negative, astigmatic lens. However, the bulging end faces of the rod give a positive lens which partially offsets this. Not all of the length of the rod is free to expand because it is constrained by the amplifier head it is mounted in, so we assume only the end-sections expand. The effective length of the expanding section of the rod varies from one laser to another depending on the way the rod is held. Our estimates give focal lengths of >10 m when the rod is pumped at 5 Hz. The thermal lens should increase linearly with thermal load, unless energy transfer upconversion is significant, in which case a stronger thermal lens increasing nonlinearly with pump power would be expected [8]. We have carried out initial

measurements of thermal lensing in the first amplifier, using a Phasics SID4 wavefront sensor. These confirm that at 5 Hz operation , the focal length of the thermal lens is well over 10 m.

Optical gating

We have chosen and ordered a BBO Pockels cell and driver from Leysop to produce a flat-top 1.55 μs pulse-train from the ~250 μs macropulses. The accelerator requirements dictate rise and fall times of just 2 – 3 ns. The Pockels cell must also be designed to handle the high average power and capable of producing a flat-top output pulse. We have chosen a BBO Pockels cell because it combines high power handling and low piezo-electric effect. However, the incident average power when the amplifiers run at the full 50 Hz repetition rate will be in excess of 2 $kWcm^{-2}$, which is high even for BBO. We propose to use an acousto-optic modulator (AOM) to dump as much excess power as possible before the Pockels cell. Fused silica AOMs have high laser damage thresholds and very low thermal and photo-elastic induced birefringence, so should provide very stable transmission. The AOM will be switched on to dump the excess power in the macropulse before and after the selected 1.5 μs pulse–train period and off during the pulse, relaxing the requirements on stability of the rf. BBO requires high operating voltages, so the chosen solution uses two crystals in series to halve the working voltage. The stability of the voltage produced by the Pockels cell driver is specified as 5% within 20 ns of switch-on and 1% during the flat-topped pulse. The ringing in the voltage at switch-on should be fixed pulse-to-pulse, so we are considering the option of using an arbitrary waveform generator and secondary Pockels cell to compensate for this as part of the stabilization scheme.

Conclusions

High power diode-pumped Nd:YLF amplifiers running in quasi steady state mode, based on a common concept of pump head geometry, have been designed and developed. We have measured output powers in excess of 3.3 kW after three passes of the amplifier. The design is based on quasi-steady state operation because of the high stability required, and the measured output reaches the steady-state after ~300 μs. Calculations based on a simplified model show good agreement with experimental results, giving us a good guideline for further development and optimization of laser performance. Assembly of the second amplifier is in progress.

We acknowledge the support of the European Community-Research Infrastructure Activity under the FP6 "Structuring the European Research Area" programme (CARE, contract number RII3-CT-2003-506395).

References

1. M.Divall, G.J.Hirst, I.N.Ross, H.Braun, R.Losito, L.Rinolfi, G.Suberlucq, *'Provision of the CTF3 Photoinjector laser oscillator'*, CARE-Report-05026-PHIN.
2. I.N.Ross, M.Csatari and S.Hutchins, *'High performance diode pumped Nd:YLF amplifier'*, Appl. Opt. **42**, 1040-1047, (2003).
3. I.N.Ross and M.Csatari CLF Annual Report 2001/2002 202-205 (2002)
4. I. Will, A. Liero, D. Mertins, W. Sandner, '*Feedback-stabilised ND:YLF amplifier system for generation of picosecond pulse trains of an exactly rectangular envelope'*, IEE J Quant Elec **34** 2020 (1998).
5. J.E.Murray, *"Pulsed gain and thermal lensing of Nd:$LiYF_4$"*, IEEE J Quant Elec **19** 488 (1983).
6. W.Koechner, *"Solid-State Laser Engineering"*, Springer.
7. M.Pollnau, P.J.Hardman, M.A.Kern, W.A.Clarkson and D.C.Hanna, *"Upconversion-induced heat generation and htermal lensing in Nd:YLF and Nd:YAG"*, Phys Rev B **58** 16076 (1998).
8. P.J.Hardman et al, *"Energy-transfer upconversion and thermal lensing in high-power end-pumped Nd:YLF laser crystals"*, IEEE J Quant Elec **35** 647 (1999).